Supporting Information

KN95 and N95 Respirators retain Filtration Efficiency despite a Loss of Dipole Charge during Decontamination

Wonjun Yim[1], Diyi Cheng[1], Shiv H. Patel[3,4], Rui Kou[5], Ying Shirley Meng[1,2], and Jesse V. Jokerst[1,2,6] *

[1]Materials Science and Engineering Program
[2]Department of Nanoengineering
[3]School of Medicine Simulation Training Center
[4]Division of Biological Sciences
[5]Department of Structural Engineering
[6]Department of Radiology
University of California, San Diego 9500 Gilman Drive, La Jolla, CA 92093, United States

* Correspondence and requests for materials should be addressed to jjokerst@ucsd.edu

Table S1. Layer thickness of N95 and KN95 respirators. The average thickness and the standard deviation were calculated using digital calipers including five measurements for each model. Material information is provided by the manufacturers.

Respirator		Model	Layer thickness (mm)				Material
			Inner	Cotton	Filter	Outer	
N95	NIOSH-approved	1. 3M 1860	0.48 ± 0.68		1.88 ± 0.06	0.29 ± 0.07	Outer(SB Polypropylene) Filter(MB Polypropylene) Inner(SB Polyester)
		2. 3M 8210	1.26 ± 0.14		1.63 ± 0.17	0.15 ± 0.02	Outer(SB Polyester) Filter(MB Polypropylene) Inner(SB Polyester)
		3. 3M 8511	0.13 ± 0.02		1.61 ± 0.11	1.33 ± 0.06	Outer(SB Polypropylene) Filter(MB Polypropylene) Inner(SB Polyester)
KN95	EUA-approved	1. Decopro	0.24 ± 0.02	1.69 ± 0.09	0.3 ± 0.02	0.15 ± 0.03	Outer(SB fabric) Filter(MB fabric) Middle(cotton) Inner(SB fabric)
		2. Powecom	0.29 ± 0.01	2.12 ± 0.04	0.23 ± 0.04	0.14 ± 0.03	Outer(SB fabric) Filter(MB fabric) Middle(hot-air cotton) Inner(SB fabric)
	Non-EUA-approved	3. SupplyAID	0.2 ± 0.22	1.83 ± 1.85	0.29 ± 0.26	0.2 ± 0.22	Outer(SB fabric) Filter(MB fabric) Middle(hot-air PP cotton) Inner(SB fabric)
		4. Yomasi	0.11 ± 0.02	2.44 ± 0.06	0.26 ± 0.02	0.27 ± 0.02	Outer(SB fabric) Filter(MB fabric) Middle(hot-air cotton) Inner(SB fabric)

Table S2. Dipole charge density of PET and paper. Dipole charge density of polyethylene (PET) and paper were measured by using voltmeter Trek Model 344. Paper is known to have no dipole charges. The PET results are comparable with prior works[1-2] that used the pulsed electroacoustic (PEA) method.

Material	Set Grid voltage (kV)	Measured dipolar voltage (kV)	Measured standard deviation (kV)	**Dipolar charge density (mC/m^2)**	Dipolar charge density deviation (mC/m^2)	**Dipolar charge density (mC/m^2)**	Reference
PET	2.5	2.4954	0.0089	0.5570	0.0020	0.37	[1]
						0.32	[2]
Paper	2.5	0.002	0.0009	0.0004	0.0002	0	

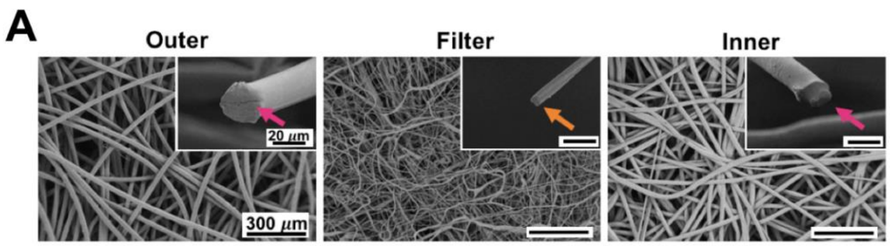

N95 (3M 1860)	Outer layer	Filter layer	Inner layer
Fiber diameter	27.07 ± 3.64	2.79 ± 0.95	24.464 ± 5.18

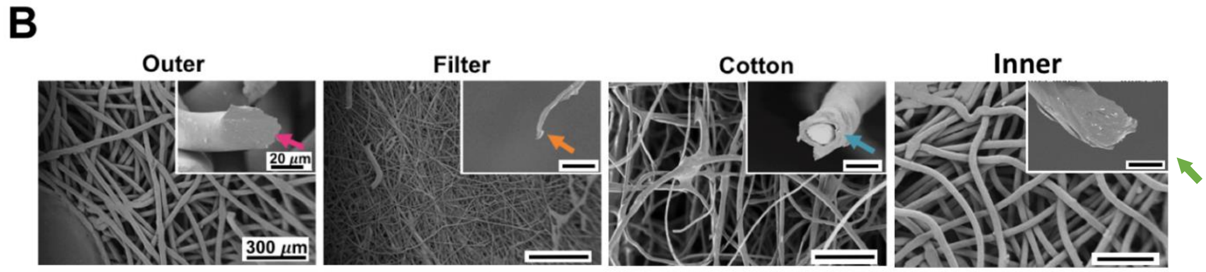

KN95 (Yomasi)	Outer layer	Filter layer	Cotton layer	Inner layer
Fiber diameter	26.07 ± 3.63	3.23 ± 1.28	22.97 ± 4.12	31.07 ± 2.10

Figure S1. Fiber diameter of (A) N95 (3M1860) and (B) KN95 (Yomasi). Fibers in the filter layer are 10-fold smaller than fibers in other layers. Each arrow shows cross-sectional area of fiber diameter in the outer, cotton, filter, and inner layers. Blue arrow indicates fibers having a core-shell structure in the cotton layer. Fiber diameter was measured by Image J software. The average size and standard deviation were calculated from five measurements. All scale bars represent 300 μm for the main SEM images and 20 μm for the inset SEM images.

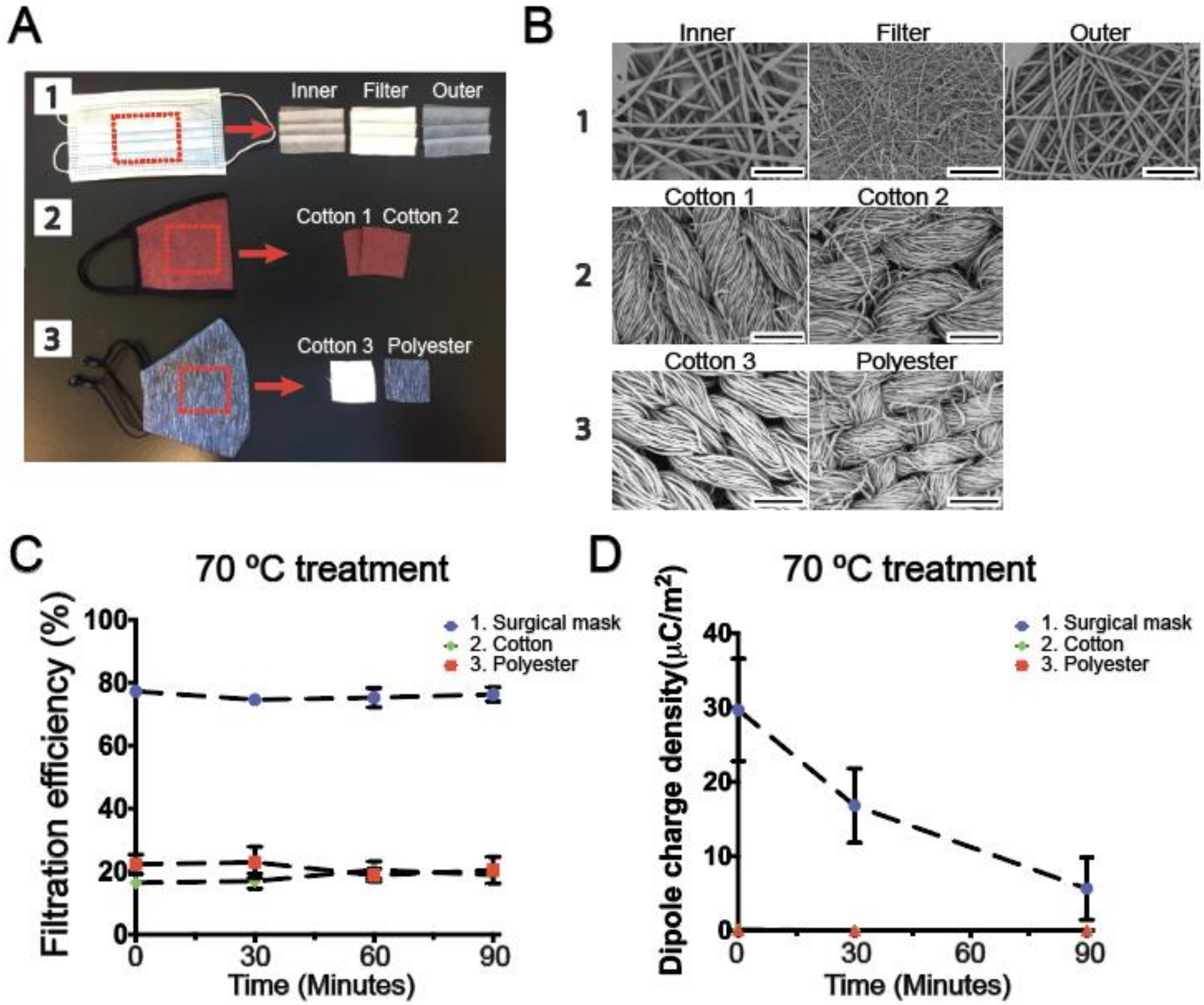

Figure S2. Commonly available commercial masks. (A) 1: Surgical mask, 2: Cotton mask, and 3: Polyester mask. Red-dotted squares and red arrows indicate the area of the mask that was removed for further analysis. (B) Cotton and polyester masks have no filter layers and consist of woven fibers. All scale bars represent 300 μm. (C) Cotton and polyester masks have 70% lower filtration efficiency than N95 respirators. (D) There are no dipole charges imposed on the cotton and polyester masks. The error bars represent the standard deviation of five measurements.

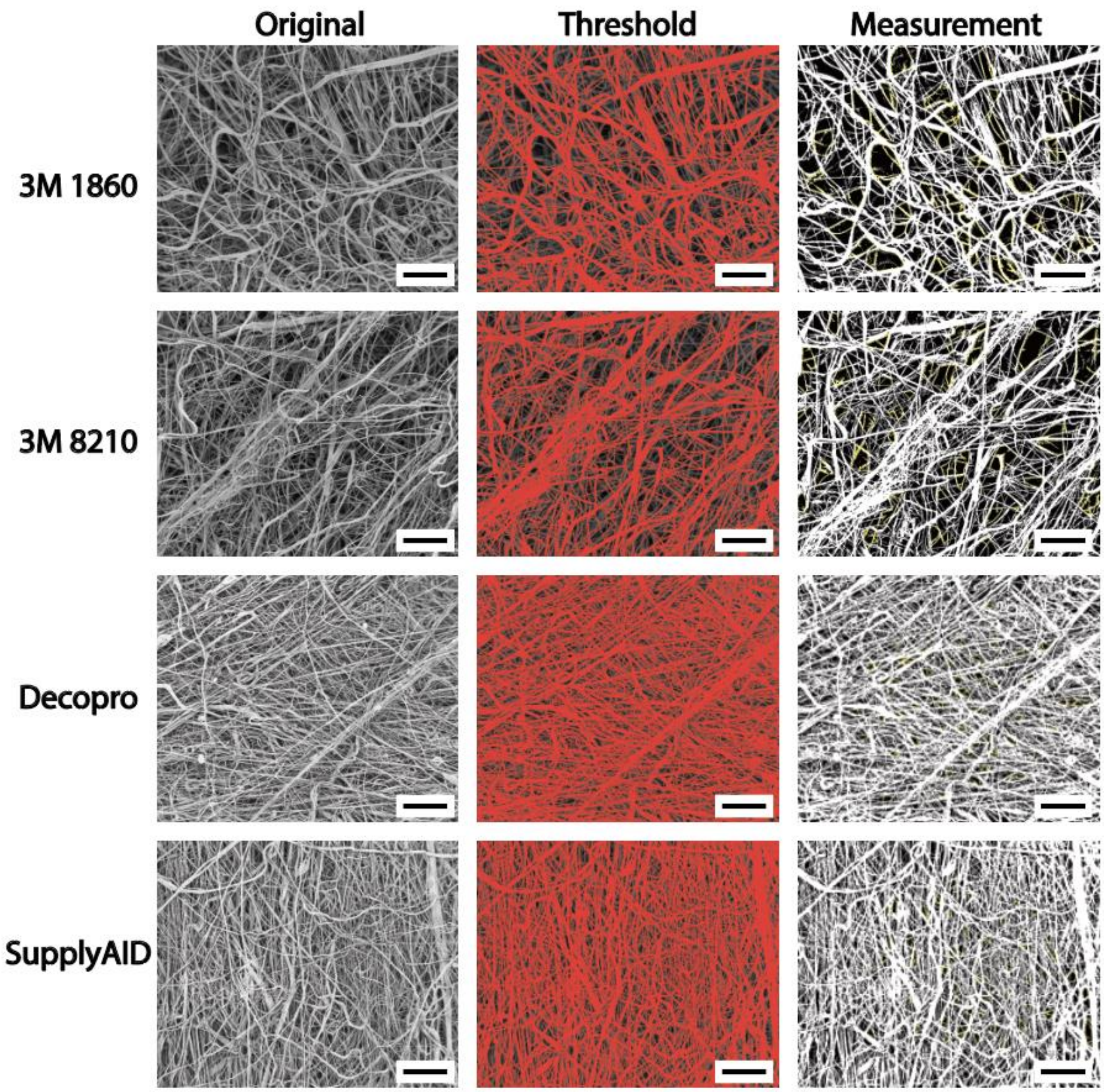

Figure S3. Pore-area size measurement. SEM images of the filter layer was converted to black (pore) and white (MB fibers) using the 'Threshold' function of Image J software. The average pore-area size was calculated from 20 measurements. All scale bars represent 300 μm.

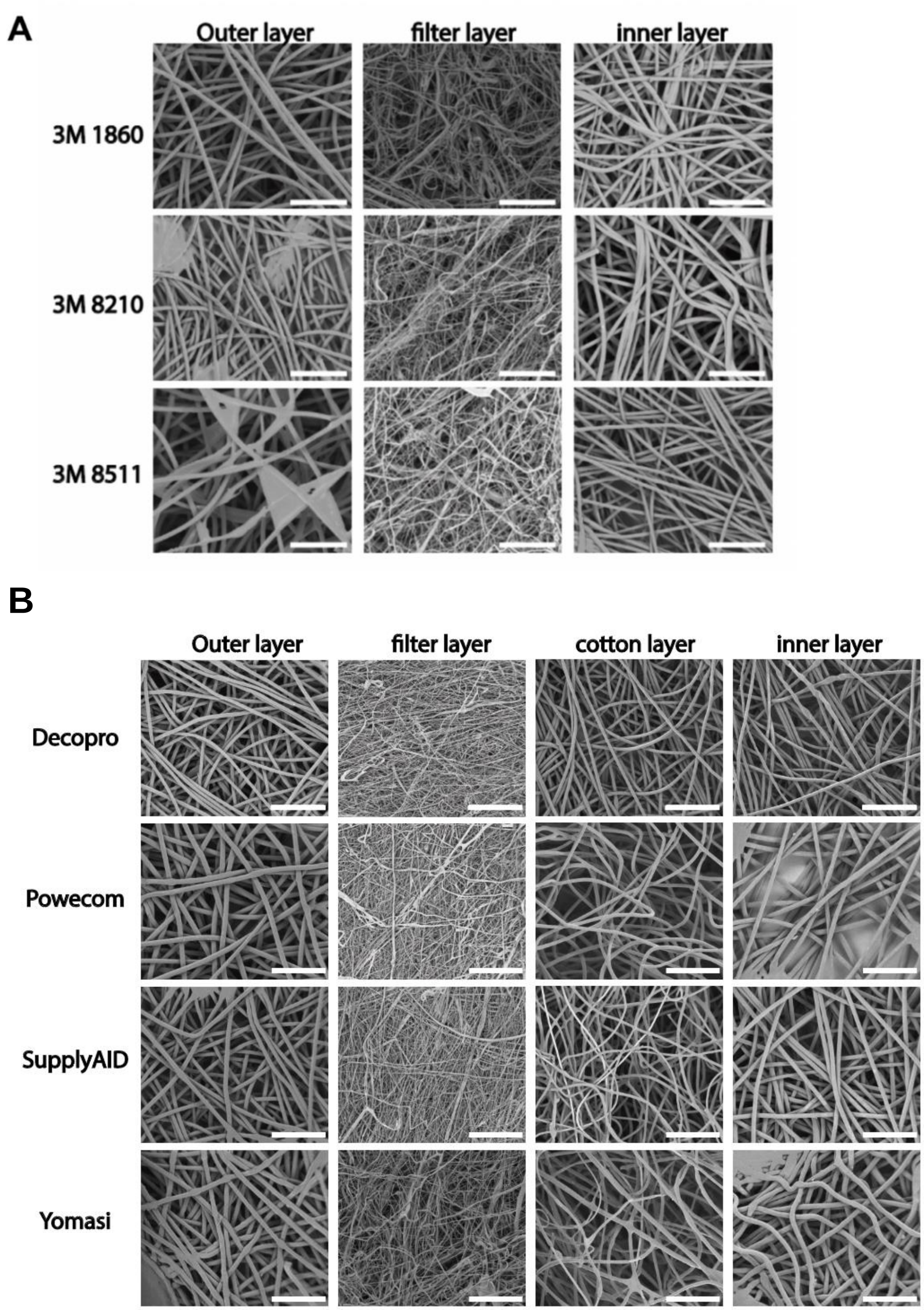

Figure S4. SEM images of each layer in N95 and KN95 respirators. (A) 3M1860, 3M 8210, and 3M 8511 are N95 respirators. (B) Decopro, Powecom, SupplyAID, and Yomasi are KN95 respirators. All N95 respirators consist of outer, filter and inner layers. All KN95 respirators are made of outer, filter, cotton, and inner layers. The filter layer in both respirators has the smallest pore-area in each layer. All scale bars represent 300 μm.

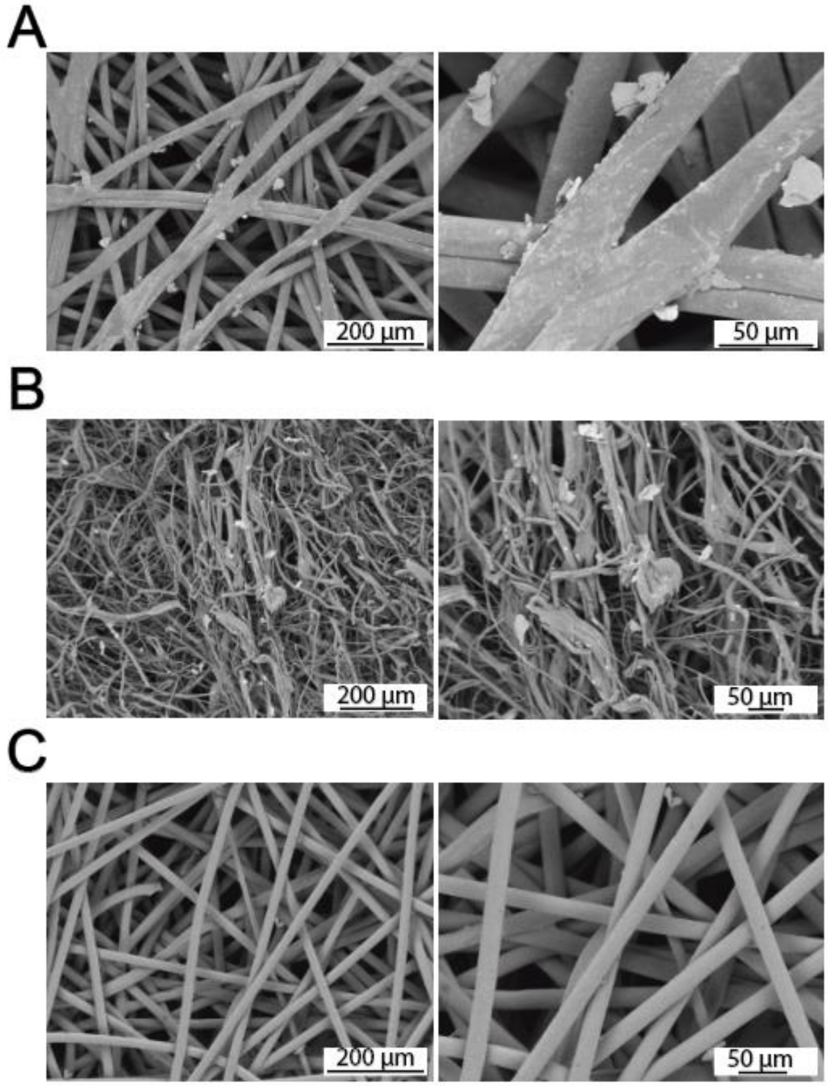

Figure S5. SEM images of each layer after filtration efficiency test. (A) Outer layer, (B) filter layer, and (C) inner layer of N95 (3M 1860). Large and small particles are attached on the SB and MB fibers.

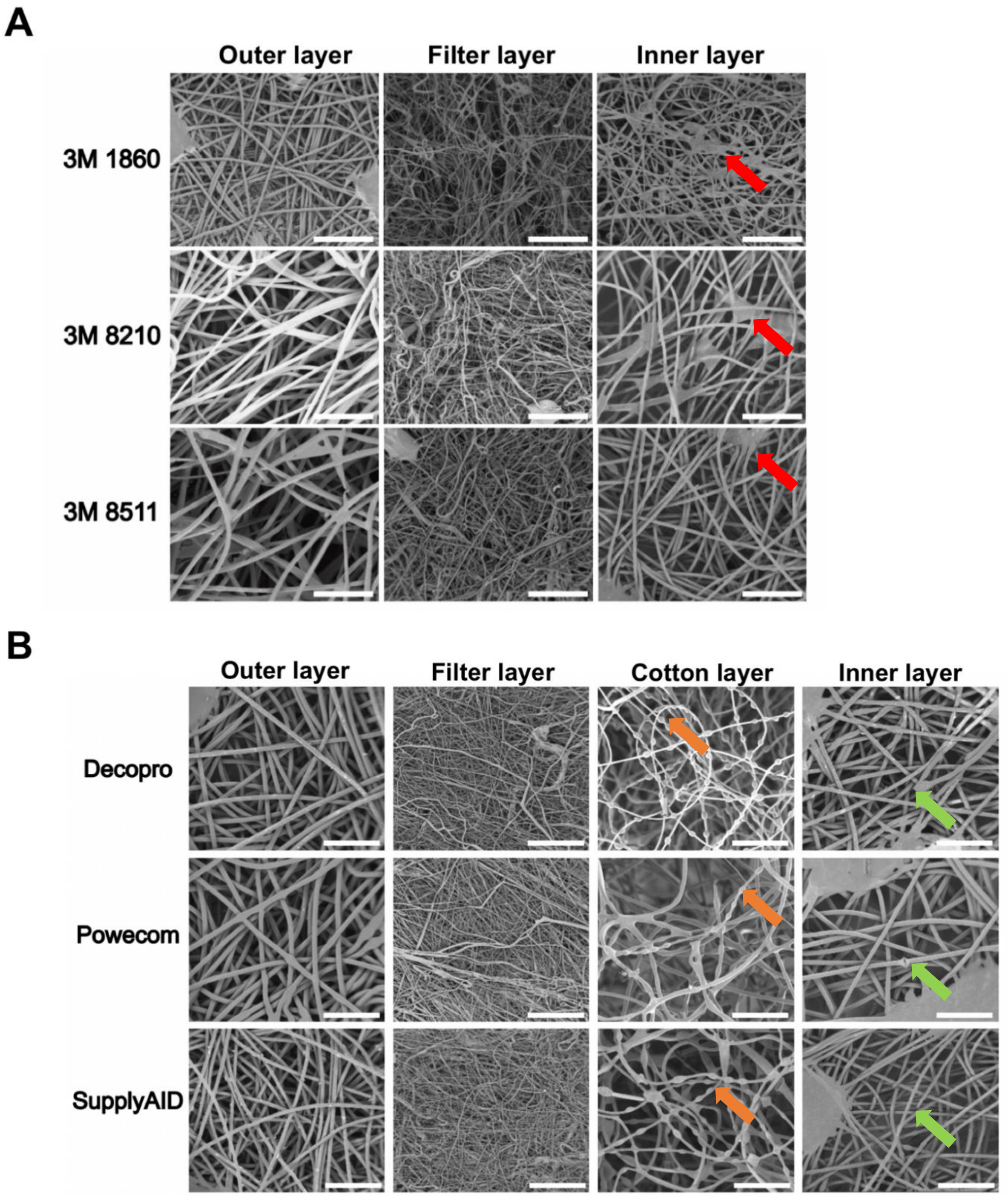

Figure S6. Fiber integrity of N95 and KN95 respirators after 150 °C treatments. (A) 3M 1860, 3M 8210, and 3M 8511 are N95 respirators**.** Red arrows indicate that the inner layer of N95 respirators melts when heated at 150 °C. (B) Decopro, Powecom, and SupplyAID are KN95 respirators. Orange arrows show fiber expansions in the cotton layer of KN95 respirators, and Green arrows indicate a fracture in the inner layer of KN95 respirators when heated at 150 °C. All scale bars represent 300 μm.

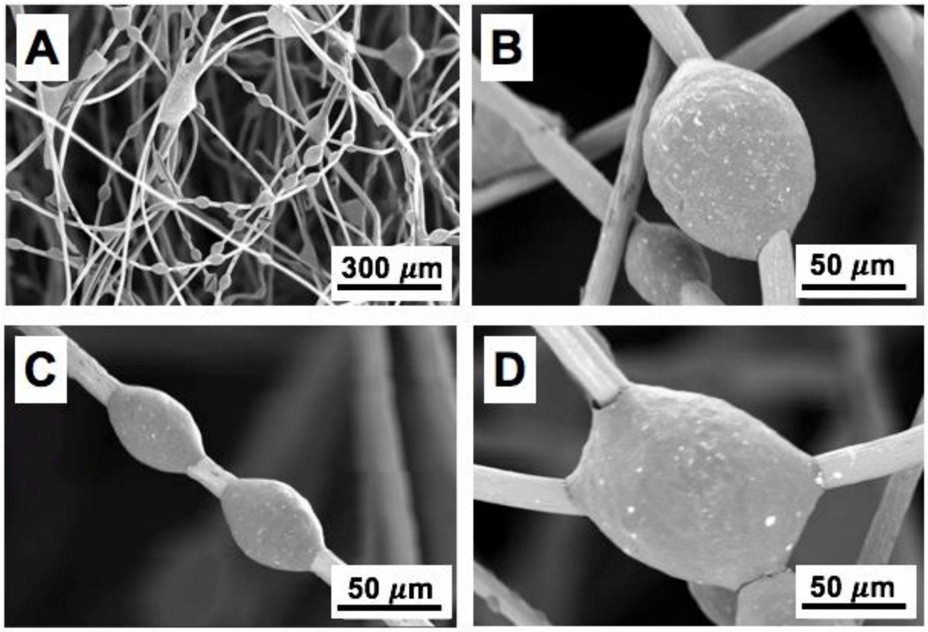

Figure S7. A balloon-shaped fiber expansion in KN95 respirator (Yomasi). (A) The cotton layer of KN95 after 150 °C treatment, (b) single expansion, (c) binary expansion, and (d) expansion at the fiber intersection.

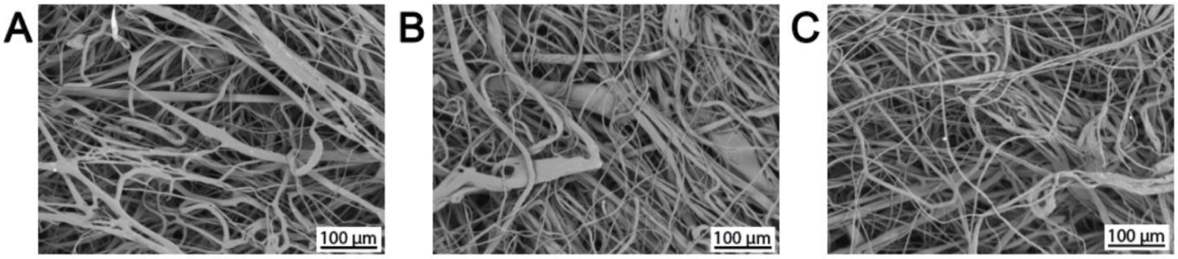

D

IPA Treatment	3M 1860	3M 8210	3M 8511
BEFORE	1.88 ± 0.06	1.63 ± 0.17	1.61 ± 0.11
AFTER	1.87 ± 0.05	1.10 ± 0.09	1.41 ± 0.09

Figure S8. SEM images and thickness of N95 respirators after IPA treatment. Fiber integrity of the filter layer in (A) 3M 1860, (B) 3M 8210, and (C) 3M 8511 after IPA treatment. (D) No thickness shrinkage occurs in the filter layers of N95 respirators before and after IPA treatment. The average size and standard deviation were calculated from five measurements.

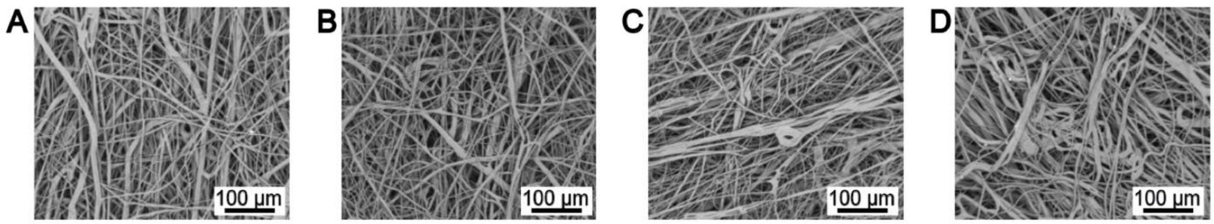

E

IPA Treatment	DECOPRO	POWECOM	SUPPLYAID	YOMASI
BEFORE	0.3 ± 0.02	0.23 ± 0.04	0.29 ± 0.26	0.26 ± 0.02
AFTER	0.3 ± 0.02	0.24 ± 0.03	0.28 ± 0.01	0.22 ± 0.02

Figure S9. SEM images and thickness of KN95 after IPA treatment. Fiber integrity of the filter layer in (A) Decopro, (B) Powecom, (C) SupplyAID, and (D) Yomasi after IPA treatment. (E) No thickness shrinkage occurs in the filter layers of KN95 respirators before and after IPA treatment. The average size and standard deviation were calculated from five measurements.

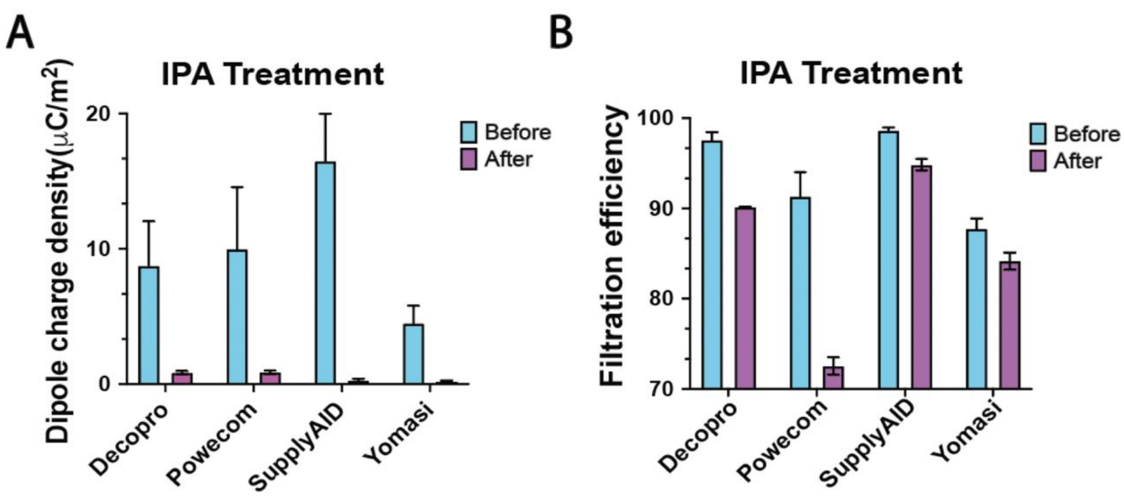

Figure S10. Dipole charge density and filtration efficiency of KN95 after IPA treatment. (A) Charge-free KN95 respirators. (B) Filtration efficiencies of KN95 respirators after IPA treatment. The error bars represent the standard deviation of five measurements.

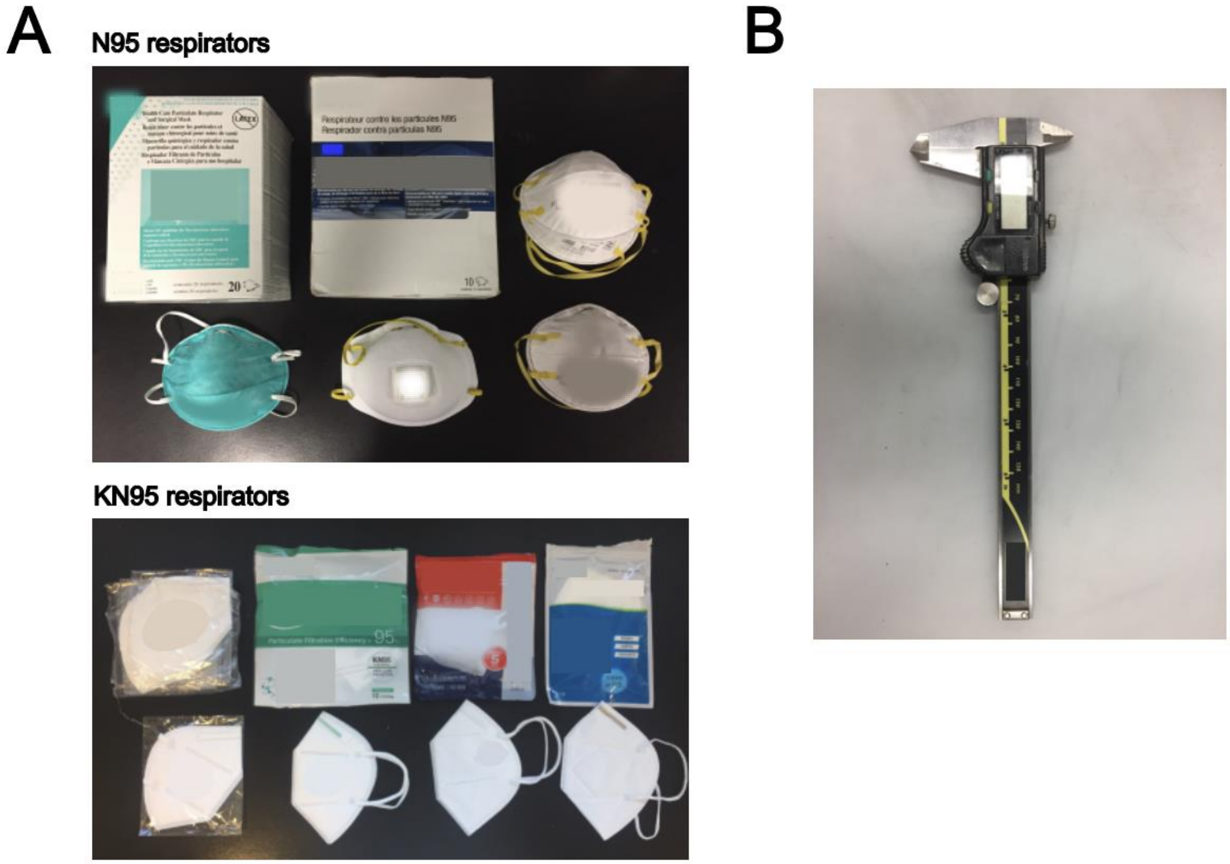

Figure S11. Material information and calibrator. (A) N95 and KN95 respirators. (B) Digimatic digital calipers were used to measure the thickness of the outer, filter, cotton, and inner layers.

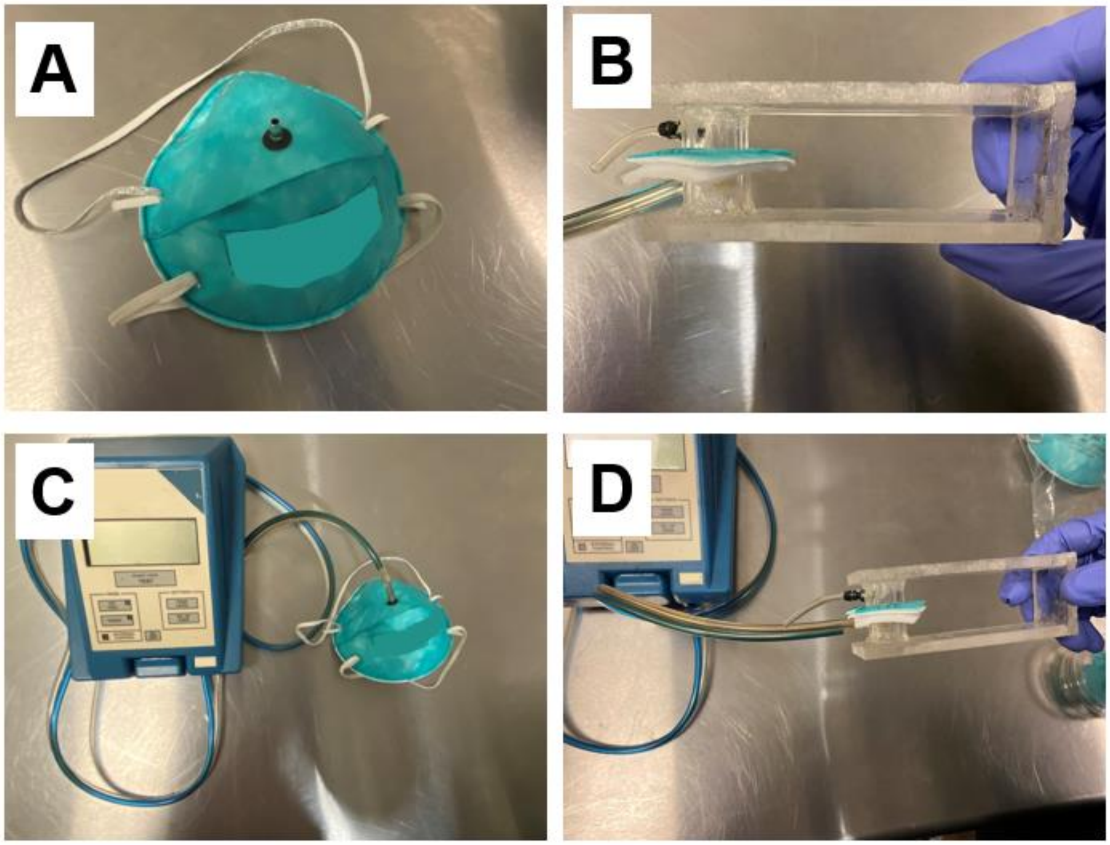

Figure S12. Filtration test of N95 respirator. (A) Sample preparation for fit factor test. (B) Sample preparation for filtration test. (C) Sample connection with the machine for measuring fit factor. (D) Sample connection with the PortaCount machine to measure filtration efficiency.

Fit factor (FF)

Fit factor (FF) is defined as the particle concentration outside the respirator divided by the particle concentration inside respirator. The instrument (PortaCount) automatically calculates the fit factor via Equation 1:[55]

$$FF = \frac{C_B + C_A}{2C_R} \quad (1)$$

Where:
FF: Fit factor
C_B: particle concentration in the ambient sample before the respirator sample
C_A: particle concentration in the ambient sample after the respirator sample
C_R: particle concentration in the respirator sample

Reference

(1) Xu, Z.; Zhang, L.; Chen, G. Decay of Electric Charge on Corona Charged Polyethylene. *Journal of Physics D: Applied Physics* **2007,** *40* (22), 7085.
(2) Xu, Z.; Zhang, L.; Chen, G. In *Measurement and Analysis of Electric Potential Decay in Corona Charged Low-Density Polyethylene Films*, 2007 IEEE International Conference on Solid Dielectrics, IEEE: 2007; pp 454-457.